

A FINITE VOLUME SCHEME FOR DIFFUSION EQUATIONS ON DISTORTED QUADRILATERAL MESHES

ZHIQIANG SHENG and GUANGWEI YUAN

Laboratory of Computational Physics, Institute of Applied Physics and
Computational Mathematics, Beijing, China

A finite volume scheme is discussed for discretizing diffusion operators. Both cell-center unknowns and cell-vertex unknowns are used originally in the construction of the finite volume scheme. Then cell-vertex unknowns are eliminated by expressing them locally as linear combinations of cell-center unknowns, which is derived by the following process. First we construct a special control-volume for each cell-vertex and then design a finite volume scheme in this control-volume to obtain a linear relation between cell-vertex unknowns and cell-center unknowns. Hence cell-vertex unknown can be expressed by the combination of neighboring cell-center unknowns, and the resulting scheme has only cell-center unknowns like standard finite difference methods. Specially, the scheme can naturally treat problems with discontinuous coefficients. Its another advantage is that highly distorted meshes can be used without the numerical results being altered remarkably. We prove theoretically that the finite volume scheme is stable and has first-order accuracy on distorted meshes. Moreover, we have tested the scheme on a few elliptic and parabolic equations. Numerical results exhibit the good behavior of our scheme.

Keywords: Finite volume scheme, Diffusion equation, Distorted mesh, Control volume, Convergence

1. Introduction

Investigating the numerical schemes with high accuracy for diffusion equations on distorted meshes is very important in

Received 5 September 2007; Accepted 22 April 2008.

The authors thank Dr. Xudeng Hang for fruitful discussions.

The project is supported by the Special Funds for Major State Basic Research Projects 2005CB321703, the National Nature Science Foundation of China (No. 60533020, 10801018).

Address correspondence to Zhiqiang Sheng, Laboratory of Computational Physics, Institute of Applied Physics and Computational Mathematics, P.O. Box 8009 Beijing, 100088, Beijing, P.R. China. E-mail: szqdxxy@163.com

Lagrangian hydrodynamics and magnetohydrodynamics. Like the finite element method and the finite difference method, the finite volume method is a discretization technique for solving partial differential equations (PDEs), which is obtained by integrating the PDE over a control volume, and it represents in general the conservation of certain physical quantity of interest, such as mass, momentum, or energy. Due to this natural association, the finite volume method is widely used in practical problems such as radiation hydrodynamics. Moreover, it is flexible enough to be applied to complex space domains, and because it works directly on the physical domain rather than on the computational domain through coordinate transformations, it can be easily used with adaptive mesh strategies.

There are many articles on the finite volume method. A finite volume scheme solving diffusion equations on nonrectangular meshes is introduced in Li et al. (1980), which is reduced to the so-called nine-point scheme on arbitrary quadrilateral meshes. This scheme has only cell-center unknowns in which each cell-vertex unknown is expressed by the simple algorithmic average of neighboring cell-center unknowns. Numerical experiments show that it loses significant accuracy on moderately and highly skewed meshes. In Wu et al. (2003) this nine-point scheme is further discussed by introducing a weighted combination with the weighted coefficients determined by the least-square minimization of the truncation error. A similar scheme for the stationary diffusion equation has been developed in Hermeline (2000) and Huang et al. (1998) In Hermeline (2000), a finite volume scheme is constructed both at the cell center and the cell vertex (i.e., the center of dual mesh) of primary mesh, hence it has both cell-center and cell-vertex unknowns. This finite volume scheme cannot be applied directly to diffusion problems with discontinuous coefficients due to the use of dual mesh. Numerical experiments show that this scheme has indeed second accuracy, but it doesn't give the theoretical proof. In Huang et al. (1998) a continuous edge flux scheme is proposed that is closely related to the Taylor series expansion scheme, and no theoretical analysis of the scheme is given there. We discussed in Yuan et al. (2007) the convergence of the scheme of Hermeline (2000) and further extended the construction of scheme to the diffusion problems with discontinuous coefficients and nonstationary diffusion problems. The

scheme in Kershaw (1981) is based on a smooth mapping between the logical mesh coordinates and the spatial ones, which gives a nine-point scheme on structured quadrilateral meshes. However, it is not conservative and suffers the loss of significant accuracy on moderately and highly skewed meshes. The MDHW scheme in Morel et al. (1992) has face-center unknowns in addition to cell-center unknowns, and the resulting diffusion matrix is asymmetric. The support-operators method (SOM) in Shashkov and Steinberg (1995), Morel et al. (1998), Lipnikov et al. (2006), Klausena and Russell (2004), Shashkov (1996) generally has both cell-center and face-center unknowns or has a dense diffusion matrix, and especially no explicit expression for the normal flux is given. In Lipnikov et al. (2006), Breil and Maire (2007) a new cell-centered diffusion scheme on two-dimensional unstructured meshes is proposed in which two normal fluxes and two temperatures on each face are at first introduced. Then a local variational formulation on each corner cell and the continuity of the normal fluxes on each face around a cell-vertex are used to obtain a cell-centered scheme. The method of multipoint flux approximations (MPFA) Aavatsmark (2002), Aavatsmark and Eigestad (2006), and Aavatsmark et al. (1998), whose discrete flux is defined on the sub-edge, obtains explicit discrete flux expression by solving a small scale linear system and often leads to a nonsymmetric coefficient matrix for general quadrilateral meshes. Shashkov (1996), Klausena and Russell (2004) presents the relationships among some locally conservative discretization methods.

In this article we present a new method of eliminating cell-center unknowns in the finite volume scheme for discretizing general diffusion operators. First we construct a special control-volume for each cell-vertex, and then devise a finite volume scheme in this control-volume to obtain a linear relation between cell-vertex unknowns and cell-center unknowns. In this way cell-vertex unknowns are expressed by the weighted combination of neighboring cell-center unknowns with the weighted coefficients being determined explicitly. Hence, only cell-center unknowns remain in the resulting diffusion scheme, and it has a local stencil. Specially, this method can naturally treat the problems with discontinuous coefficients. Moreover, compared with the SOM and MPFA method, it keeps the advantage of simplicity and straightforward figure. We will prove that this method is stable and

first-order convergent. Moreover, it is extended to nonstationary diffusion problems.

The rest of the article is organized as follows. In Sec. 2, we describe the construction of the finite volume scheme for stationary diffusion problems on distorted quadrilateral meshes. In Sec. 3, we prove that our scheme is stable and has first-order accuracy. In Sec. 4, we extend the results to nonstationary diffusion problems. Then we present some numerical examples to show its performance on several test problems in Sec. 5. Finally, in Sec. 6 we end with some concluding remarks.

2. Construction of Finite Volume Scheme

2.1. Problem and Notation

Consider the stationary diffusion equation:

$$-\nabla \cdot (\kappa \cdot \nabla u) = f \quad \text{in } \Omega, \quad (2.1)$$

$$u(x) = 0 \quad \text{on } \partial\Omega, \quad (2.2)$$

where Ω is an open bounded polygonal set of R^2 with boundary $\partial\Omega$.

In this article, we will denote cells by K, L, \dots , and corresponding cell-centers also by K, L, \dots , and cell-vertex by A, B, \dots , and cell sides by σ (see Figure 1). If one cell side σ is a common edge of cells K and L , and its vertices are A and B , then we denote

$$\sigma = K/L = BA.$$

Let \mathcal{J} be the set of all the cells, which are assumed to be quadrilateral. Let ε be the set of all the cell sides, ε_{int} the set of all the cell sides not on $\partial\Omega$, ε_{ext} the set of all the cell sides on $\partial\Omega$, and ε_K be the set of all the cell sides of cell K . Denote $h = (\sup_{K \in \mathcal{J}} m(K))^{1/2}$, or $h = \sup_{K \in \mathcal{J}} \text{diam}(K)^{1/2}$, where $m(K)$ is the area of cell K , and $\text{diam}(K)$ is the diameter of cell K .

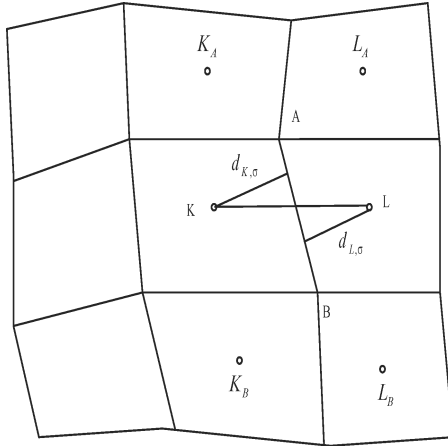


FIGURE 1 The mesh stencil.

2.2. Finite Volume Scheme on Cell-Center

Integrate (2.1) over the cell \$K\$, to obtain

$$\sum_{\sigma \in \mathcal{E}_K} F_{K,\sigma} = \int_K f(x) dx, \tag{2.3}$$

where the continuous flux on the edge \$\sigma\$ is

$$\mathcal{F}_{K,\sigma} = - \int_{\sigma} \kappa(x) \nabla u(x) \cdot \vec{n}_{K,\sigma} dl, \tag{2.4}$$

where \$\vec{n}_{K,\sigma}\$ is the unit outer normal on the edge \$\sigma\$ of cell \$K\$ (see Figure 2).

In Figure 2, \$\vec{\tau}_{BA}\$ and \$\vec{\tau}_{KI}\$ are unit vectors along the directions \$BA\$ and \$KI\$ respectively, \$I\$ is the intersect point of \$BA\$ and \$KI\$, and \$\theta_{\sigma}\$ is the angle between \$\vec{n}_{K,\sigma}\$ and \$\vec{\tau}_{KI}\$. Noticing that

$$\vec{n}_{K,\sigma} = - \tan \theta_{\sigma} \vec{\tau}_{BA} + \frac{1}{\cos \theta_{\sigma}} + \vec{\tau}_{KI},$$

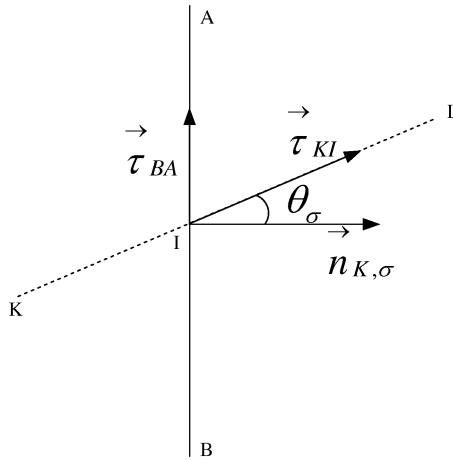


FIGURE 2 The unit vectors on side σ .

we can write the continuous flux as

$$\mathcal{F}_{K,\sigma} = \tan \theta_\sigma \int_\sigma \kappa(x) \nabla u(x) \cdot \vec{\tau}_{BA} dl - \frac{1}{\cos \theta_\sigma} \int_\sigma \kappa(x) \nabla u(x) \cdot \vec{\tau}_{KI} dl. \tag{2.5}$$

By the Taylor expansion, one has

$$u(I) - u(K) = \nabla u(x) \cdot (I - K) + \int_0^1 (H_I - H_K) r dr,$$

$$u(A) - u(B) = \nabla u(x) \cdot (A - B) + \int_0^1 (H_A - H_B) r dr,$$

where $H_I = (\nabla^2 u(rx + (1-r)I)(I-x)I-x)$, and $\nabla^2 u(rx + (1-r)I)$ is the Hessian matrix of u at the point $rx + (1-r)I$, $x \in \sigma$. The other notations H_K, H_A and H_B have the similar definition. Hence,

$$\int_\sigma \kappa(x) \nabla u(x) \cdot \vec{\tau}_{KI} dl = \frac{|A-B|}{|I-K|} \kappa_{K,\sigma} (u(I) - u(K)) - \frac{\int_\sigma \left(\kappa(x) \int_0^1 (H_I - H_K) r dr \right) dl}{|I-K|},$$

$$\int_{\sigma} \kappa(x) \nabla v(x) \cdot \vec{\tau}_{BA} dl = \kappa_{K,\sigma} (u(A) - u(B)) - \frac{\int_{\sigma} \left(\kappa(x) \int_0^1 (H_A - H_B) r dr \right) dl}{|A - B|},$$

where $\kappa_{K,\sigma}$ is the line integral average of $\kappa(x)$ over τ in cell K .

Substitute the above two equations into (2.5) to obtain

$$\mathcal{F}_{K,\sigma} = -\tau_{K,\sigma} (u(I) - u(K) - D_{K,\sigma} (u(A) - u(B))) + R_{K,\sigma} \quad (2.6)$$

where $\tau_{K,\sigma} = \frac{|A-B|}{|I-L| \cos \theta_{\sigma}} \kappa_{K,\sigma}$, $D_{K,\sigma} = \frac{\sin \theta_{\sigma} |I-K|}{|A-B|}$, and $R_{K,\sigma} = O(h^2)$.

Similarly, we have

$$\mathcal{F}_{L,\sigma} = -\tau_{L,\sigma} (u(I) - u(L) - D_{L,\sigma} (u(D) - u(A))) + R_{L,\sigma}, \quad (2.7)$$

where $\tau_{L,\sigma} = \frac{|A-B|}{|I-L| \cos \theta_{\sigma}} \kappa_{L,\sigma}$, $D_{L,\sigma} = \frac{\sin \theta_{\sigma} |I-L|}{|A-B|}$, $R_{L,\sigma} = O(h^2)$ and $\kappa_{L,\sigma}$ is the line integral average of $\kappa(x)$ over σ in cell L .

Using the continuous condition of edge normal flux $\mathcal{F}_{K,\sigma} = -\mathcal{F}_{L,\sigma}$, we get

$$\begin{aligned} u(I) &= \frac{1}{\tau_{K,\sigma} + \tau_{L,\sigma}} (\tau_{K,\sigma} u(K) + \tau_{L,\sigma} u(L)) \\ &\quad + (\tau_{K,\sigma} D_{K,\sigma} - \tau_{L,\sigma} D_{L,\sigma}) (u(A) - u(B)) \\ &\quad + \frac{1}{\tau_{K,\sigma} + \tau_{L,\sigma}} (R_{K,\sigma} + R_{L,\sigma}). \end{aligned} \quad (2.8)$$

Substitute (2.8) into (2.6) to obtain

$$\mathcal{F}_{K,\sigma} = -\tau_{\sigma} (u(L) - u(K) - D_{\sigma} (u(A) - u(B))) + \bar{R}_{K,\sigma}, \quad (2.9)$$

where $\tau_{\sigma} = \frac{\tau_{K,\sigma} \tau_{L,\sigma}}{\tau_{K,\sigma} + \tau_{L,\sigma}}$, $D_{\sigma} = \frac{(I-K, A-B)}{|A-B|^2}$, $\bar{R}_{K,\sigma} = \frac{\tau_{L,\sigma} R_{K,\sigma} - \tau_{K,\sigma} R_{L,\sigma}}{\tau_{K,\sigma} + \tau_{L,\sigma}}$

Similarly, we have

$$\mathcal{F}_{L,\sigma} = -\tau_{\sigma} (u(K) - u(L) - D_{\sigma} (u(B) - u(A))) + \bar{R}_{L,\sigma}, \quad (2.10)$$

where $\bar{R}_{L,\sigma} = \frac{\tau_{K,\sigma} R_{L,\sigma} - \tau_{L,\sigma} R_{K,\sigma}}{\tau_{K,\sigma} + \tau_{L,\sigma}} = -\bar{R}_{K,\sigma}$.

2.3. The Expression of Cell-Vertex Unknowns

The values of u at A and B appear in the expression of flux (2.9) and (2.10). To calculate $u(A)$, we first construct a special control volume K' for the cell-vertex A . Two different cases are distinguished according to the size of the angle between two adjacent lines connecting the cell-center with the cell-vertex, which is shared by the neighboring cells. Case 1 is that all these angles with the vertex A are less than 180° , hence it forms a control volume $CDEF$ for the cell-vertex A (see Figure 3). In Case 2, there has a angle—e.g., $\angle L_A AK_A$ —which is larger than or equal to 180° , hence it forms a control volume $CDEFGA$ (see Figure 4). In Case 1, we require that $CD \perp AK_A$, $DE \perp AK$, $EF \perp AL$ and $FC \perp AL_A$. In Case 2, $CD \perp AK_A$, $DE \perp AK$, $EF \perp AL$ and $FG \perp AL_A$ also are required.

2.3.1. CASE 1

At first, we consider Case 1. Integrate (2.1) over the cell K' (the quadrilateral $CDEF$), to obtain

$$\sum_{\sigma \in \mathcal{E}_{K'}} \mathcal{F}_{A,\sigma} = \int_{K'} f(x) dx \tag{2.11}$$

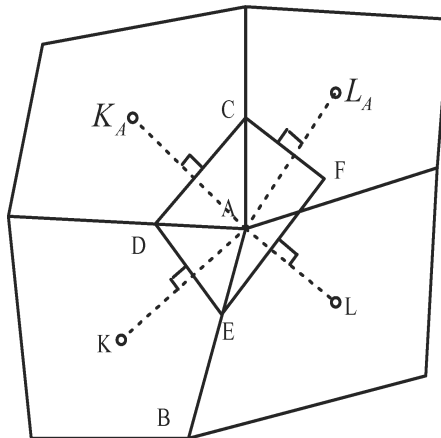


FIGURE 3 Case 1: All angles are less than 180° .

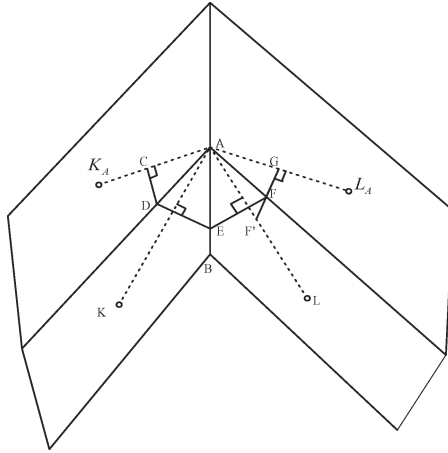


FIGURE 4 Case 2: One angle is larger than or equal to 180°.

where the continuous flux on the edge σ is

$$\mathcal{F}_{A,\sigma} = - \int_{\sigma} \kappa(x) \nabla u(x) \cdot \vec{n}_{A,\sigma} dl, \tag{2.12}$$

where $\vec{n}_{A,\sigma}$ is the unit outer normal on the edge σ of cell K' (see Figure 3).

Using the Taylor expansion, we have

$$u(K_A) - u(A) = \nabla u(x) \cdot (K_A - A) + \int_0^1 (H_{K_A} - H_A) r dr, \quad x \in \sigma = CD.$$

Hence, for $\sigma = CD$,

$$\begin{aligned} \int_{\sigma} \kappa(x) \nabla u(x) \cdot \vec{n}_{K',\sigma} dl &= \frac{\kappa_{K',\sigma} |C - D|}{|K_A - A|} (u(K_A) - u(A)) \\ &\quad - \frac{1}{|K_A - A|} \int_{\sigma} \kappa(x) \left(\int_0^1 (H_{K_A} - H_A) r dr \right) dl, \end{aligned} \tag{2.13}$$

where $\kappa_{K',\sigma}$ is the line integral average of $\kappa(x)$ over σ in the cell K' . Denote $R_{K',\sigma} = -\frac{1}{|K_A - A|} \int_{\sigma} \kappa(x) \left(\int_0^1 (H_{K_A} - H_A) r dr \right) dl$. It's obvious that there holds $|R_{K',\sigma}| = O(h^2)$.

Substitute (2.13) into (2.12) to obtain

$$\mathcal{F}_{A,\sigma} = \frac{\kappa_{K',\sigma} |C - D|}{|K_A - A|} (u(K_A) - u(A)) + R_{K',\sigma}, \quad \sigma = CD. \quad (2.14)$$

In a similar way, we can obtain the normal flux on the other sides,

$$\begin{aligned} \mathcal{F}_{A,DE} &= -\frac{\kappa_{K'DE} |D - E|}{|K - A|} (u(K) - u(A)) + R_{K'DE}, \\ \mathcal{F}_{A,EF} &= -\frac{\kappa_{K'EF} |E - F|}{|L - A|} (u(L) - u(A)) + R_{K'EF}, \\ \mathcal{F}_{A,FC} &= -\frac{\kappa_{K'FC} |F - C|}{|L_A - A|} (u(L_A) - u(A)) + R_{K'FC}. \end{aligned}$$

Substitute the above four equations into (2.11) to obtain

$$\begin{aligned} &-\tau_{CD}(u(K_A) - u(A)) - \tau_{DE}(u(K) - u(A)) - \tau_{EF}(u(L) - u(A)) \\ &-\tau_{FC}(u(L_A) - u(A)) + R_{K'} = \int_{K'} f(x) dx, \end{aligned} \quad (2.15)$$

where

$$\begin{aligned} \tau_{CD} &= \frac{\kappa_{K',CD} |C - D|}{|K_A - A|}, \quad \tau_{DE} = \frac{\kappa_{K',DE} |D - E|}{|K - A|}, \quad \tau_{EF} = \frac{\kappa_{K',EF} |E - F|}{|L - A|}, \\ \tau_{FC} &= \frac{\kappa_{K',FC} |F - C|}{|L_A - A|}, \quad R_{K'} = R_{K',CD} + R_{K',DE} + R_{K',EF} + R_{K',FC}. \end{aligned}$$

By (2.15), we get

$$\begin{aligned} u(A) &= \omega_{A_1} u(K_A) + \omega_{A_2} u(K) + \omega_{A_3} u(L) \\ &+ \omega_{A_4} u(L_A) + b_A f(A) + R_A, \end{aligned} \quad (2.16)$$

where

$$\begin{aligned} \omega_{A_1} &= \frac{\tau_{CD}}{\tau_{CD} + \tau_{DE} + \tau_{EF} + \tau_{FC}}, & \omega_{A_2} &= \frac{\tau_{DE}}{\tau_{CD} + \tau_{DE} + \tau_{EF} + \tau_{FC}}, \\ \omega_{A_3} &= \frac{\tau_{EF}}{\tau_{CD} + \tau_{DE} + \tau_{EF} + \tau_{FC}}, & \omega_{A_4} &= \frac{\tau_{FC}}{\tau_{CD} + \tau_{DE} + \tau_{EF} + \tau_{FC}}, \end{aligned}$$

$$b_A = \frac{m(K')}{\tau_{CD} + \tau_{DE} + \tau_{EF} + \tau_{FC}}, \quad R_A = \frac{-R_{K'}}{\tau_{CD} + \tau_{DE} + \tau_{EF} + \tau_{FC}}.$$

It's obvious that $b_A = O(h^2)$, $R_A = O(h^2)$, $0 < \omega_{A_i} < 1$, and $\sum_{i=1}^4 \omega_{A_i} = 1$.

Similarly, one has

$$u(B) = \omega_{B_1} u(K) + \omega_{B_2} u(K_B) + \omega_{B_3} u(L_B) + \omega_{B_4} u(L) + b_B f(b) + R_B, \tag{2.17}$$

where $b_B = O(h^2)$, $R_B = O(h^2)$, $0 < \omega_{B_i} < 1$, and $\sum_{i=1}^4 \omega_{B_i} = 1$.

2.3.2. CASE 2

Now we consider Case 2. Integrate (2.1) over the cell K' ($CDEFGA$), to obtain

$$\sum_{\sigma \in \mathcal{E}_{K'}} \mathcal{F}_{A,\sigma} = \int_{K'} f(x) dx, \tag{2.18}$$

Proceeding the same derivation as in Case 1, we can obtain the expression of the flux on the sides CD , DE , EF , and FG as follows:

$$\mathcal{F}_{A,CD} = -\frac{\kappa_{K',CD} |C - D|}{|K_A - A|} (u(K_A) - u(A)) + R_{K',CD}, \tag{2.19}$$

$$\mathcal{F}_{A,DE} = -\frac{\kappa_{K',DE} |D - E|}{|K - A|} (u(K_A) - u(A)) + R_{K',DE}, \tag{2.20}$$

$$\mathcal{F}_{A,EF} = -\frac{\kappa_{K',EF} |E - F|}{|L - A|} (u(L) - u(A)) + R_{K',EF}, \tag{2.21}$$

$$\mathcal{F}_{A,FG} = -\frac{\kappa_{K',FG} |F - G|}{|L_A - A|} (u(L_A) - u(A)) + R_{K',FG}, \tag{2.22}$$

For the flux on the sides GA , one has

$$\mathcal{F}_{A,GA} = -\frac{\kappa_{K',GA} |G - A|}{|G - F|} (u(G) - u(F)) + R'_{K',GA}, \tag{2.23}$$

where $R'_{K',GA} = O(h^2)$. In the expression of $\mathcal{F}_{A,GA}$, $u(G)$ and $u(F)$ are unknowns. We should get their values by interpolation, and the interpolation accuracy must be at least $O(h^2)$. The values of

$u(G)$ and $u(F)$ can be obtained by using the linear interpolation of the values at A , L and L_A , e.g.,

$$u(G) = \frac{|G - L_A|}{|A - L_A|} u(A) + \frac{|G - A|}{|A - L_A|} u(L_A) + O(h^2). \tag{2.24}$$

If the cells L_A and L are homogeneous, we have

$$u(F) = \omega_{F_1} u(A) - \omega_{F_2} u(L) + \omega_{F_3} u(L_A) + O(h^2), \tag{2.25}$$

where ω_{F_i} ($i = 1, 2, 3$) satisfy the following relation,

$$\begin{cases} \omega_{F_1} + \omega_{F_2} + \omega_{F_3} = 1 \\ x_{AF}\omega_{F_1} - x_{LF}\omega_{F_2} + x_{L_A F}\omega_{F_3} = 0, \\ y_{AF}\omega_{F_1} + y_{LF}\omega_{F_2} + y_{L_A F}\omega_{F_3} = 0 \end{cases} \tag{2.26}$$

where $x_{AF} = x_A - x_F$, $y_{AF} = y_A - y_F$, and the others have similar definition (Yuan and Sheng, 2007).

If the cells L_A and L are inhomogeneous, using the continuous condition of edge normal flux $F_{L,AF} = -F_{L_A,AF}$, we can get a similar equation with (2.8) that is

$$\begin{aligned} u(F) = & \frac{1}{\tau_{L,AF} + \tau_{L_A,AF}} (\tau_{L,sAF} u(F') + \tau_{L_A,AF} u(G)) \\ & + (\tau_{L,AF} D_{L,AF} - \tau_{L_A,AF} D_{L_A,AF})(u(A) - u(F)) + O(h^2) \end{aligned} \tag{2.27}$$

Denote F' be the intersect point of AL and GF . Obviously,

$$u(F') = \frac{|F' - L|}{|A - L|} u(A) + \frac{|F' - A|}{|A - L|} u(L) + O(h^2). \tag{2.28}$$

Combine (2.24)–(2.28) to find ω'_{F_i} ($i = 1, 2, 3$) such that

$$u(F) = \omega'_{F_1} u(A) + \omega'_{F_2} u(L) + \omega'_{F_3} u(L_A) + O(h^2). \tag{2.29}$$

Substitute (2.24) and (2.25) or (2.29) into (2.23) to obtain some coefficients $\omega'_i (i = 1, 2, 3)$ such that

$$\mathcal{F}_{A,GA} = -\frac{\kappa_{K',GA} |G - A|}{|G - F|} (\omega'_1 u(A) + \omega'_2 u(L) + \omega'_3 u(L_A)) + R_{K',GA}, \tag{2.30}$$

where $R_{K',GA} = O(h^2)$. Also, one has

$$\begin{aligned} \mathcal{F}_{A,AC} = & -\frac{\kappa_{K'AC} |A - C|}{|C - D|} (\omega''_1 u(A) + \omega''_2 u(K_A) + \omega''_3 u(K)) \\ & + R_{K',AC}, \end{aligned} \tag{2.31}$$

where $\omega'' (i = 1, 2, 3)$ are obtained similarly and $R_{K',AC} = O(h^2)$.

Substituting (2.19)–(2.22), (2.30) and (2.31) into (2.18), and doing some algebraic operations, we obtain

$$\begin{aligned} u(A) = & \omega_{A_1} u(K_A) + \omega_{A_2} u(K) + \omega_{A_3} u(L) + \omega_{A_4} u(L_A) \\ & + b_A f(A) + R_A, \end{aligned} \tag{2.32}$$

where $R_A = O(h^2)$. It's obvious that there are similar expressions of $u(A)$ and $u(B)$ for Case 1 and Case 2; hence we will consider only Case 1 in the rest of this article.

2.3.3. ANOTHER CONTROL VOLUME

For Case 1, we can form another control volume (see Figure 5). Here $C, D, E,$ and F lie on the grid line, and there hold $CD \perp AK_A, DE \perp AK, EF \perp AL,$ and $FC \perp AL'_A$.

It's obvious that the flux $\mathcal{F}_{A,CD}, \mathcal{F}_{A,DE},$ and $\mathcal{F}_{A,EF}$ have the same expressions as in Case 1 of the Subsection 2.3.1, and

$$\mathcal{F}_{A,FC} = -\frac{\kappa_{K'FC} |F - C|}{|L'_A - A|} (u(L'_A) - u(A)) + R'_{K'FC}. \tag{2.33}$$

In the above expression of $\mathcal{F}_{A,FC}$, the value of $u(L'_A)$ is unknown. From the same method as in Case 2 we can derive the expression of $\mathcal{F}_{A,FC}$ and it follows that the expression of $u(A)$ is obtained.

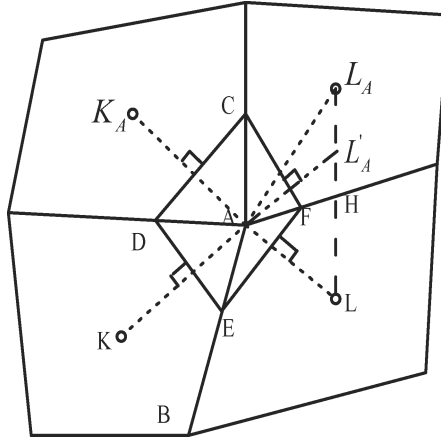


FIGURE 5 Another control volume.

2.4. Finite Volume Scheme

Substituting (2.16) and (2.17) into (2.9), we have

$$\begin{aligned} \mathcal{F}_{K,\sigma} = & -\tau_\sigma (u(L) - u(K) - D_\sigma (\omega_{A_1} u(K_A) + \omega_{A_2} u(K) \\ & + \omega_{A_3} u(L) - \omega_{A_4} u(L_A) + b_A f(A) - (\omega_{B_1} u(K) + \omega_{B_2} u(K_B) \\ & + \omega_{B_3} u(K_B) + \omega_{B_4} u(L) + b_B f(B)))) + W_{K,\sigma}, \end{aligned}$$

where $\tau_\sigma = \frac{\kappa_{K,\sigma}|A-B|}{\cos\theta_\sigma|K-L|}$, $D_\sigma = \frac{(K-L, A-B)}{|A-B|}$, and $W_{K,c} = O(h^2)$. Denote

$$\begin{aligned} \bar{F}_{K,\sigma} = & -\tau_\sigma (u(L) - u(K) - D_\sigma (\omega_{A_1} u(K_A) + \omega_{A_2} u(K) \\ & + \omega_{A_3} u(L)\omega_{A_4} u(L_A) + b_A f(A) - (\omega_{B_1} u(K) \\ & + \omega_{B_2} u(K_B)\omega_{B_3} u(L_B) + \omega_{B_4} u(L) + b_B f(B))). \end{aligned}$$

Therefore, $\mathcal{F}_{K,\sigma} = \bar{F}_{K,\sigma} + W_{K,\sigma}$.

For $\sigma = K|L = BA \in \varepsilon_{int}$, let

$$\begin{aligned} F_{K,\sigma} = & -\tau_\sigma (u_L - u_K - D_\sigma (\omega_{A_1} u_{K_A} + \omega_{A_2} u_K + \omega_{A_3} u_L + \omega_{A_4} u_{L_A} \\ & - (\omega_{B_1} u_K + \omega_{B_2} u_{K_B} + \omega_{B_3} u_{L_B} + \omega_{B_4} u_L))) \\ & + \tau_\sigma D_\sigma (b_A f_A - b_B f_B). \end{aligned} \tag{2.34}$$

For $\sigma = BA \in \varepsilon_{ext} \cap \varepsilon_K$, let

$$F_{K,\sigma} = \tau_\sigma u_K, \tag{2.35}$$

where $\tau_\sigma = \frac{\kappa_{K,\sigma}|A-B|}{|I-K|\cos\theta_\sigma}$ and $I = \frac{B+A}{2}$ is the mid-point of BA.

The finite volume scheme of the problem (2.1)–(2.2) is defined as follows:

$$\sum_{\sigma \in \varepsilon_K} F_{K,\sigma} = f_K m(K), \quad \text{for } K \in \mathcal{J}, \tag{2.36}$$

$$u_A = u_B = u_I = 0, \quad \text{for } \sigma = BA \in \varepsilon_{ext} \tag{2.37}$$

where $f_K = f(K)$.

This scheme often leads to a nonsymmetric coefficient matrix for general quadrilateral meshes. When the mesh line are orthogonal, the scheme reduces to the standard five-point scheme. It is straightforward to extend this method on quadrangles meshes to arbitrary polygon meshes.

3. Stability and Convergence of Finite Volume Scheme

In order to obtain the theorems of stability and convergence, we introduce the following assumptions.

(H1): There is a given constant $\varepsilon_0 \in (0,1)$ and a small constant $\varepsilon > 0$ satisfying $\varepsilon_0 + \varepsilon < 1$ such that

$$\begin{aligned} \tau_\sigma D_\sigma^2 \omega_{A_1}^2 &\leq \frac{1 - \varepsilon_0 - \varepsilon}{16} \tau_{K_A|K}, & \tau_\sigma D_\sigma^2 \omega_{A_4}^2 &\leq \frac{1 - \varepsilon_0 - \varepsilon}{16} \tau_{L_A|L}, \\ \tau_\sigma D_\sigma^2 \omega_{B_2}^2 &\leq \frac{1 - \varepsilon_0 - \varepsilon}{16} \tau_{K|K_B}, & \tau_\sigma D_\sigma^2 \omega_{B_3}^2 &\leq \frac{1 - \varepsilon_0 - \varepsilon}{16} \tau_{L|L_B}, \\ D_\sigma (\omega_{A_3} + \omega_{A_4} - \omega_{B_3} - \omega_{B_4}) &\leq \frac{\varepsilon_0}{2}. \end{aligned}$$

(H2): Assume that there exists a constant C such that for any $K \in \mathcal{J}$ and the control volume K' constructed at any vertex of K

(see the Subsection 2.3)

$$\frac{1}{C} \leq \frac{m(K)}{m(K')} \leq C.$$

The above assumption (H1) implies a geometric constraint on cell deformation. For any orthogonal mesh, there holds $D_\sigma = 0$ for any $\sigma \in \varepsilon$. When κ is a constant, there has $\tau_\sigma = \frac{\kappa|A-B|}{|K-L|\cos\theta_\sigma}$, $D_\sigma = \frac{(L-K, A-B)}{|A-B|^2} = \frac{|L-K|\sin\theta_\sigma}{|A-B|}$. It is obvious that the assumption $\frac{\tau_\sigma}{\tau_{K_A}|K}|D_\sigma^2\omega_{A_1}^2 \leq \frac{1-\varepsilon_0-\varepsilon}{16}$ is a constraint on the geometric parameters, which include the size of the angle between the cell side and the segment connecting neighboring cell-centers and the ratio between the length of cell side and the length of segment connecting neighboring cell-centers.

3.1. Stability

Now we prove that our scheme (2.36)–(2.37) is stable.

Theorem 3.1. *Assume (H1) and (H2) are satisfied. Then there exists a constant C , independent of h , such that for the solution of (2.36)–(2.37) there holds following inequality*

$$\sum_{\sigma \in \varepsilon} \tau_\sigma (u_L - u_K)^2 \leq C \sum_{K \in \mathcal{J}} |f_K|^2 m(K).$$

Proof. Making the scalar product of u_K with (2.36) and summing up the resulting products for $K \in \mathcal{J}$, we get

$$\sum_{K \in \mathcal{J}} \sum_{\sigma \in \varepsilon_K} F_{K,\sigma} u_K = \sum_{K \in \mathcal{J}} f_K u_K m(K). \tag{3.1}$$

Notice that

$$\begin{aligned} \sum_{K \in \mathcal{J}} \sum_{\sigma \in \varepsilon_K} F_{K,\sigma} u_K &= - \sum_{K \in \mathcal{J}} \sum_{\sigma \in \varepsilon_K} \tau_\sigma (u_L - u_K - D_\sigma (\omega_{A_1} u_{K_A} + \omega_{A_2} u_K \\ &\quad + \omega_{A_3} u_L + \omega_{A_4} u_{L_A} - (\omega_{B_1} u_K + \omega_{B_2} u_{K_B} + \omega_{B_3} u_{L_B} \\ &\quad + \omega_{B_4} u_L))) u_K + \sum_{K \in \mathcal{J}} \sum_{\sigma \in \varepsilon_K} \tau_\sigma D_\sigma (b_A f_A - b_B f_B) u_K \end{aligned}$$

$$\begin{aligned}
 &= \sum_{\sigma \in \mathcal{E}} \tau_{\sigma} (u_L - u_K)^2 + \sum_{\sigma \in \mathcal{E}} \tau_{\sigma} D_{\sigma} (\omega_{A_1} u_{K_A} + \omega_{A_2} u_K \\
 &\quad + \omega_{A_3} u_L + \omega_{A_4} u_{L_A} - (\omega_{B_1} u_K + \omega_{B_2} u_{K_B} + \omega_{B_3} u_{L_B} \\
 &\quad + \omega_{B_4} u_L)) (u_K - u_L) + \sum_{\sigma \in \mathcal{E}} \tau_{\sigma} D_{\sigma} (b_A f_A - b_B f_B) \\
 &\quad \times (u_K - u_L) \\
 &= \sum_{\sigma \in \mathcal{E}} \tau_{\sigma} (u_L - u_K)^2 + \sum_{\sigma \in \mathcal{E}} \tau_{\sigma} D_{\sigma} (\omega_{A_1} (u_{K_A} - u_K) \\
 &\quad + \omega_{A_4} (u_{L_A} - u_L) + \omega_{B_2} (u_K - u_{K_B}) + \omega_{B_3} (u_L - u_{L_B}) \\
 &\quad + (\omega_{A_2} + \omega_{A_1} + \omega_{B_1} - \omega_{B_2}) u_K \\
 &\quad + (\omega_{A_3} + \omega_{A_4} + \omega_{B_3} - \omega_{B_4}) u_L) (u_K - u_L) \\
 &\quad + \sum_{\sigma \in \mathcal{E}} \tau_{\sigma} D_{\sigma} (b_A f_A - b_B f_B) (u_K - u_L) \\
 &= \sum_{\sigma \in \mathcal{E}} \tau_{\sigma} (u_L - u_K)^2 + \sum_{\sigma \in \mathcal{E}} \tau_{\sigma} D_{\sigma} (\omega_{A_1} (u_{K_A} - u_K) \\
 &\quad + \omega_{A_4} (u_{L_A} - u_L) + \omega_{B_2} (u_K - u_{K_B}) \\
 &\quad + \omega_{B_3} (u_L - u_{L_B})) (u_K - u_L) \\
 &\quad - \sum_{\sigma \in \mathcal{E}} \tau_{\sigma} D_{\sigma} (\omega_{A_3} + \omega_{A_4} - \omega_{B_3} - \omega_{B_4}) (u_K - u_L)^2 \\
 &\quad + \sum_{\sigma \in \mathcal{E}} \tau_{\sigma} D_{\sigma} (b_A f_A - b_B f_B) (u_K - u_L). \tag{3.2}
 \end{aligned}$$

Substituting (3.2) into (3.1), we obtain

$$\begin{aligned}
 &\sum_{\sigma \in \mathcal{E}} \tau_{\sigma} (u_L - u_K)^2 - \sum_{\sigma \in \mathcal{E}} \tau_{\sigma} D_{\sigma} (\omega_{A_3} + \omega_{A_4} - \omega_{B_3} - \omega_{B_4}) (u_K - u_L)^2 \\
 &\quad + \sum_{\sigma \in \mathcal{E}} \tau_{\sigma} D_{\sigma} [\omega_{A_1} (u_{K_A} - u_K) + \omega_{A_4} (u_{L_A} - u_L) + \omega_{B_2} (u_K - u_{K_B}) \\
 &\quad + \omega_{B_3} (u_L - u_{L_B})] (u_K - u_L) \tag{3.3} \\
 &= \sum_{K \in \mathcal{J}} f_K u_K m(K) - \sum_{\sigma \in \mathcal{E}} \tau_{\sigma} D_{\sigma} (b_A f_A - b_B f_B) (u_K - u_L).
 \end{aligned}$$

By the Cauchy inequality and (3.3),

$$\begin{aligned} & \sum_{\sigma \in \mathcal{E}} \tau_{\sigma} (u_L - u_K)^2 - \sum_{\sigma \in \mathcal{E}} \tau_{\sigma} D_{\sigma} (\omega_{A_3} + \omega_{A_4} - \omega_{B_3} - \omega_{b_4}) (u_K - u_L)^2 \\ & \leq \sum_{\sigma \in \mathcal{E}} \frac{1}{2} \tau_{\sigma} (u_L - u_K)^2 + 2 \sum_{\sigma \in \mathcal{E}} \tau_{\sigma} D_{\sigma}^2 (\omega_{A_1}^2 (u_{K_A} - u_K)^2 \\ & \quad + \omega_{A_4}^2 (u_{L_A} - u_L)^2 + \omega_{B_2}^2 (u_K - u_{K_B})^2 + \omega_{B_3}^2 (u_L - u_{L_B})^2) \\ & \quad + \frac{C}{\varepsilon} \sum_{K \in \mathcal{J}} |f_K|^2 m(K) + \frac{\varepsilon}{4C} \sum_{K \in \mathcal{J}} |u_K|^2 m(K) + \frac{\varepsilon}{8} \sum_{\sigma \in \mathcal{E}} \tau_{\sigma} (u_K - u_L)^2 \\ & \quad + \frac{2}{\varepsilon} \sum_{\sigma \in \mathcal{E}} \tau_{\sigma} D_{\sigma}^2 (b_A f_A - b_B f_B)^2. \end{aligned}$$

It is easy to see the following discrete Poincaré inequality holds

$$\sum_{K \in \mathcal{J}} |u_K|^2 m(K) \leq C \sum_{\sigma \in \mathcal{E}} \tau_{\sigma} (u_L - u_K)^2.$$

From the above inequalities and the assumption (H1) it follows that for a constant $C = C(\varepsilon)$

$$\sum_{\sigma \in \mathcal{E}} \tau_{\sigma} (u_L - u_K)^2 \leq C \sum_{K \in \mathcal{J}} |f_K|^2 m(K) + C \sum_{\sigma \in \mathcal{E}} \tau_{\sigma} D_{\sigma}^2 (b_A f_A - b_B f_B)^2.$$

Note that $|b_A| \leq Cm(K') = O(h^2)$. Applying the assumption (H2) gives

$$\sum_{\sigma \in \mathcal{E}} \tau_{\sigma} (u_L - u_K)^2 \leq C \sum_{K \in \mathcal{J}} |f_K|^2 m(K).$$

Hence, our scheme is proved to be stable. □

3.2. Convergence

The Equation (2.3) is equivalent to the following equation:

$$\sum_{\sigma \in \mathcal{E}_K} F_{K,\sigma} = f_K m(K) + S_K m(K), \tag{3.4}$$

where $f_K = f(K)$, $S_K = \int_K (f(x) - f_K) dx / m(K)$. Obviously, $|S_K| \leq Ch$. Let $e_K = u(K) - u_K$ for $K \in \mathcal{J}$. Subtract (2.36) from (3.4) to obtain

$$\sum_{\sigma \in \mathcal{E}_K} G_{K,\sigma} = S_K m(K) - \sum_{\sigma \in \mathcal{E}_K} W_{K,\sigma}, \tag{3.5}$$

where $G_{K,\sigma} = \bar{F}_{K,\sigma} - F_{K,\sigma}$

We now state an error estimate for the scheme (2.36)–(2.37).

Theorem 3.2. *Assume (H1) and (H2) are satisfied. Then there exists a constant C, independent of h, such that,*

$$\left(\sum_{\sigma \in \mathcal{E}} \tau_\sigma (e_L - e_K)^2 \right)^{1/2} \leq Ch.$$

Proof. Making the scalar product of e_k with (3.5), and summing up the resulting products for $K \in \mathcal{J}$, we get

$$\sum_{K \in \mathcal{J}} \sum_{\sigma \in \mathcal{E}_K} G_{K,\sigma} e_K = \sum_{K \in \mathcal{J}} S_K e_K m(K) - \sum_{K \in \mathcal{J}} \sum_{\sigma \in \mathcal{E}_K} W_{K,\sigma} e_K. \tag{3.6}$$

Here

$$\begin{aligned} \sum_{K \in \mathcal{J}} \sum_{\sigma \in \mathcal{E}_K} G_{K,\sigma} e_K &= - \sum_{\sigma \in \mathcal{E}} \tau_\sigma D_\sigma (\omega_{A_3} + \omega_{A_4} - \omega_{B_3} - \omega_{B_4}) (e_K - e_L)^2 \\ &\quad + \sum_{\sigma \in \mathcal{E}} \tau_\sigma (e_L - e_K)^2 + \sum_{\sigma \in \mathcal{E}} \tau_\sigma D_\sigma (\omega_{A_1} (e_{K_A} - e_K) \\ &\quad + \omega_{A_4} (e_{L_A} - e_L) + \omega_{B_2} (e_K - e_{K_B}) + \omega_{B_3} (e_L - e_{L_B})) \\ &\quad \times (e_K - e_L). \end{aligned} \tag{3.7}$$

Notice that $W_{L,\sigma} = -W_{K,\sigma}$ and Denote $W_\sigma = W_{K,\sigma}$ Substitute (3.7) into (3.6) to obtain

$$\begin{aligned}
 \sum_{\sigma \in \mathcal{E}} \tau_\sigma (e_L - e_K)^2 &- \sum_{\sigma \in \mathcal{E}} \tau_\sigma D_\sigma (\omega_{A_3} + \omega_{A_4} - \omega_{B_3} - \omega_{B_4}) (e_K - e_L)^2 \\
 &+ \sum_{\sigma \in \mathcal{E}} \tau_\sigma D_\sigma (\omega_{A_1} (e_{K_A} - e_{K_A})) \\
 &+ \omega_{A_4} (e_{L_A} - e_L) + \omega_{B_2} (e_K - e_{K_B}) \\
 &+ \omega_{B_3} (e_L - e_{L_B}) (e_K - e_L) \\
 &= \sum_{K \in \mathcal{J}} S_K e_K m(K) - \sum_{\sigma \in \mathcal{E}} W_\sigma (e_K - e_L). \quad (3.8)
 \end{aligned}$$

From the Cauchy inequality and (3.8) it gives

$$\begin{aligned}
 \sum_{\sigma \in \mathcal{E}} \tau_\sigma (e_L - e_K)^2 &- \sum_{\sigma \in \mathcal{E}} \tau_\sigma D_\sigma (\omega_{A_3} + \omega_{A_4} - \omega_{B_3} - \omega_{B_4}) (e_K - e_L)^2 \\
 &\leq \sum_{\sigma \in \mathcal{E}} \frac{1}{2} \tau_\sigma (e_L - e_K)^2 + 2 \sum_{\sigma \in \mathcal{E}} \tau_\sigma D_\sigma^2 [\omega_{A_4}^2 (e_{K_A} - e_K)^2 \\
 &\quad + \omega_{A_4}^2 (e_{L_A} - e_L)^2 + \omega_{B_2}^2 (e_K - e_{K_B})^2 + \omega_{B_3}^2 (e_L - e_{L_B})]^2 \\
 &\quad + \sum_{\sigma \in \mathcal{E}} \frac{\varepsilon}{8} \tau_\sigma (e_K - e_L)^2 + \sum_{\sigma \in \mathcal{E}} \frac{2}{\varepsilon \tau_\sigma} |W_\sigma|^2 \\
 &\quad + \frac{\varepsilon}{8C_1} \sum_{K \in \mathcal{J}} |e_K|^2 m(K) + Ch^2.
 \end{aligned}$$

Applying the assumption (H1)–(H2) and the discrete Poincaré inequality, we obtain

$$\sum_{\sigma \in \mathcal{E}} \tau_\sigma (e_L - e_K)^2 \leq Ch^2.$$

The proof of Theorem 3.2 is finished. \square

4. Finite Volume Scheme for Nonstationary Diffusion Equation

Consider the construction of the following nonstationary diffusion problem:

$$u_t - \nabla \cdot (\kappa(x, t) \cdot \nabla u) = f(x, t), \quad \text{in } \Omega \cup (0, T], \quad (4.1)$$

$$u(x, t) = 0 \quad \text{on } \partial\Omega \cup (0, T], \quad (4.2)$$

$$u(x, 0) = \varphi(x) \quad \text{on } \Omega, \quad (4.3)$$

where Ω is an open bounded polygonal set of R^2 with boundary $\partial\Omega$, and $\varphi(x) = 0$ on $\partial\Omega$. We shall use some notations and symbols similar to those of stationary diffusion equation above.

Integrate (4.1) over the cell K to obtain

$$\int_K u_t dx + \sum_{\sigma \in \mathcal{E}_K} \mathcal{F}_{K,\sigma}^{n+1} = \int_K f(x, t^{n+1}) dx, \quad (4.4)$$

where the continuous normal flux on the edge σ is

$$\mathcal{F}_{K,\sigma}^{n+1} = - \int_{\sigma} \kappa(x, t^{n+1}) \nabla u(x, t^{n+1}) \cdot \vec{n}_{K,\sigma} dl. \quad (4.5)$$

By proceeding as for the stationary diffusion problem, we have

$$\begin{aligned} \mathcal{F}_{K,\sigma}^{n+1} &= -\tau_{\sigma}^{n+1} (u(L, t^{n+1}) - u(K, t^{n+1}) - D_{\sigma} (u(A, t^{n+1}) \\ &\quad - u(B, t^{n+1}))) + \bar{R}_{K,\sigma}^{n+1}, \\ \mathcal{F}_{L,\sigma}^{n+1} &= -\tau_{\sigma}^{n+1} (u(K, t^{n+1}) - u(L, t^{n+1}) - D_{\sigma} (u(B, t^{n+1}) \\ &\quad - u(A, t^{n+1}))) + \bar{R}_{L,\sigma}^{n+1}, \end{aligned}$$

where τ_{σ}^{n+1} , D_{σ} , $\bar{R}_{L,\sigma}^{n+1}$, and $\bar{R}_{K,\sigma}^{n+1}$ have similar definitions with those in the stationary diffusion problem, and there holds $\bar{R}_{K,\sigma}^{n+1} = -\bar{R}_{L,\sigma}^{n+1} = O(h^2)$. It's obvious that we need the values of $u(x, t)$ at (A, t^{n+1}) and (B, t^{n+1}) in the expression of these normal flux.

Integrate (4.1) over the cell K' (see the subsection 2.3), to obtain

$$\int_K u_t(x, t^{n+1}) dx + \sum_{\sigma \in \mathcal{E}_{K'}} \mathcal{F}_{A,\sigma}^{n+1} = \int_{K'} f(x, t^{n+1}) dx, \quad (4.6)$$

where the continuous normal flux on the edge σ is

$$\mathcal{F}_{A,\sigma}^{n+1} = - \int_{\sigma} \kappa(x, t^{n+1}) \nabla u(x, t^{n+1}) \cdot \vec{n}_{A,\sigma} dl. \quad (4.7)$$

where $\vec{n}_{A,\sigma}$ is the unit outer normal on the edge σ of cell K' . Equation (4.6) is equivalent to the following equation:

$$\frac{u(A, t^{n+1}) - u(A, t^n)}{\Delta t} m(K') + \sum_{\sigma \in \mathcal{E}_{K'}} \mathcal{F}_{A,\sigma}^{n+1} = f(A, t^{n+1}) m(K') + S_{K'}^{n+1}, \quad (4.8)$$

where $f_A^{n+1} = f(A, t^{n+1})$, $S_{K'}^{n+1} = \int_{K'} s_{K'}^{n+1}(x) dx$, and

$$s_{K'}^{n+1} = \frac{u(A, t^{n+1}) - u(A, t^n)}{\Delta t} - u_t(x, t^{n+1}) + f(x, t^{n+1}) - f(A, t^{n+1}).$$

Obviously,

$$|S_{K'}^{n+1}| \leq C(\Delta t + h) h^2.$$

Similar to the stationary diffusion problem, we have

$$\begin{aligned} \mathcal{F}_{A,CD}^{n+1} &= -\frac{\kappa_{K',CD}|C - D|}{|K_A - A|} (u(K_A, t^{n+1}) - u(A, t^{n+1})) + R_{K'CD}^{n+1}, \\ \mathcal{F}_{A,DE}^{n+1} &= -\frac{\kappa_{K',DE}|D - E|}{|K - A|} (u(K_A, t^{n+1}) - u(A, t^{n+1})) + R_{K'DE}^{n+1}, \\ \mathcal{F}_{A,EF}^{n+1} &= -\frac{\kappa_{K',EF}|E - F|}{|L - A|} (u(L_A, t^{n+1}) - u(A, t^{n+1})) + R_{K'EF}^{n+1}, \\ \mathcal{F}_{A,FC}^{n+1} &= -\frac{\kappa_{K',FC}|F - C|}{|L_A - A|} (u(L_A, t^{n+1}) - u(A, t^{n+1})) + R_{K'FC}^{n+1}, \end{aligned}$$

where $R_{K'\sigma}^{n+1} = O(h^2)$ for $\sigma = CD, DE, EF, FC$.

Substituting the above four equations into (4.8), we obtain

$$\begin{aligned}
 & \frac{u(A, t^{n+1}) - u(A, t^n)}{\Delta t} m(K') - \tau_{CD}(u(K_A, t^{n+1}) - u(A, t^{n+1})) \\
 & - \tau_{DE}(u(K, t^{n+1}) - u(A, t^{n+1})) - \tau_{EF}(u(L, t^{n+1}) - u(A, t^{n+1})) \\
 & - \tau_{FC}(u(L_A, t^{n+1}) - u(A, t^{n+1})) \\
 & = f(A, t^{n+1}) m(K') + R_{K'}^{n+1}, \tag{4.9}
 \end{aligned}$$

where

$$\begin{aligned}
 \tau_{CD} &= \frac{\kappa_{K',CD}|C - D|}{|K_A - A|}, \quad \tau_{DE} = \frac{\kappa_{K',DE}|D - E|}{|K - A|}, \\
 \tau_{EF} &= \frac{\kappa_{K',EF}|E - F|}{|L - A|}, \\
 \tau_{FC} &= \frac{\kappa_{K',FC}|F - C|}{|L_A - A|}, \quad R_{K'}^{n+1} = S_{K'}^{n+1} \\
 & - (R_{K',CD}^{n+1} + R_{K',DE}^{n+1} + R_{K',EF}^{n+1} + R_{K',FC}^{n+1}).
 \end{aligned}$$

Denote $a_A = m(K') + \Delta t (\tau_{CD} + \tau_{DE} + \tau_{EF} + \tau_{FC})$. By (4.9) we conclude that

$$\begin{aligned}
 u(A, t^{n+1}) &= \omega_{A_1} u(K_A, t^{n+1}) + \omega_{A_2} u(K, t^{n+1}) + \omega_{A_3} u(L, t^{n+1}) \\
 & + \omega_{A_4} u(L_A, t^{n+1}) + \omega_{A_0} u(A, t^n) + b_A f(A, t^{n+1}) \\
 & + R_A^{n+1}, \tag{4.10}
 \end{aligned}$$

where

$$\begin{aligned}
 \omega_{A_1} &= \frac{\Delta t \tau_{CD}}{a_A}, \quad \omega_{A_2} = \frac{\Delta t \tau_{DE}}{a_A}, \quad \omega_{A_3} = \frac{\Delta t \tau_{EF}}{a_A}, \quad \omega_{A_4} = \frac{\Delta t \tau_{FC}}{a_A}, \\
 \omega_{A_0} &= \frac{m(K')}{a_A}, \quad b_A = \frac{\Delta t m(K')}{a_A}, \quad R_A^{n+1} = \frac{\Delta t R_{K'}^{n+1}}{a_A}.
 \end{aligned}$$

It's obvious that $b_A = O(\Delta t + m(K'))$, $R_A = O(\Delta t + m(K'))$, $0 < \omega_{A_i} < 1$, and $\sum_{i=0}^4 \omega_{A_i} = 1$. Similarly, one has

$$\begin{aligned}
 u(B, t^{n+1}) &= \omega_{B_1} u(K, t^{n+1}) + \omega_{B_2} u(K_B, t^{n+1}) + \omega_{B_3} u(L_B, t^{n+1}) \\
 &\quad + \omega_{B_4} u(L, t^{n+1}) + \omega_{B_0} u(B, t^n) + b_B f(B, t^{n+1}) + R_B.
 \end{aligned}
 \tag{4.11}$$

where $b_B = O(\Delta t + m(K'))$, $R_B = O(\Delta t + m(K'))$, $0 < \omega_{B_i} < 1$, and $\sum_{i=0}^4 \omega_{B_i} = 1$.

Denote

$$\begin{aligned}
 \bar{F}_{K,\sigma}^{n+1} &= -\tau_\sigma [u(L, t^{n+1}) - u(K, t^{n+1}) - D_\sigma(\omega_{A_1} u(K_A, t^{n+1}) \\
 &\quad + \omega_{A_2} u(K, t^{n+1}) + \omega_{A_3} u(L, t^{n+1}) + \omega_{A_4} u(L_A, t^{n+1}) \\
 &\quad + \omega_{A_0} u(A, t^n) + b_A f(A, t^{n+1}) \\
 &\quad - (\omega_{B_1} u(K, t^{n+1}) + \omega_{B_2} u(K_B, t^{n+1}) + \omega_{B_3} u(L_B, t^{n+1}) \\
 &\quad + \omega_{B_4} u(L, t^{n+1}) + \omega_{B_0} u(B, t^n) + b_B f(B, t^{n+1}))].
 \end{aligned}
 \tag{4.12}$$

Therefore, $\mathcal{F}_{K,\sigma}^{n+1} = \bar{F}_{K,\sigma}^{n+1} + W_{K,\sigma}^{n+1}$, where $W_{K,\sigma}^{n+1} = O(h^2)$.

For $\sigma = K|L = BA \in \varepsilon_{int}$, let

$$\begin{aligned}
 F_{K,\sigma}^{n+1} &= -\tau_\sigma (u_L^{n+1} - u_K^{n+1} - D_\sigma(\omega_{A_1} u_{K_A}^{n+1} + \omega_{A_2} u_K^{n+1} + \omega_{A_3} u_L^{n+1} \\
 &\quad + \omega_{A_4} u_{L_A}^{n+1} + \omega_{A_0} u_A^n + b_A f_A^{n+1} - (\omega_{B_1} u_K^{n+1} + \omega_{B_2} u_{K_B}^{n+1} \\
 &\quad + \omega_{B_3} u_{L_B}^{n+1} + \omega_{B_4} u_L^{n+1} + \omega_{B_0} u_B^n + b_B f_B^{n+1}))).
 \end{aligned}
 \tag{4.13}$$

For $\sigma = BA \in \varepsilon_{ext} \cap \varepsilon$, let

$$F_{K,\sigma}^{n+1} = \tau_\sigma u_K^{n+1},
 \tag{4.14}$$

where $\tau_\sigma^{n+1} = \frac{|A-B|}{|I-K| \cos \theta_\sigma} \kappa_{K,\sigma}^{n+1}$ and $I = \frac{B+A}{2}$.

The finite volume scheme of the problem (4.1)–(4.3) is defined as follows:

$$\frac{u_K^{n+1} - u_K^n}{\Delta t} m(\kappa) + \sum_{\sigma \in \varepsilon_K} F_{K,\sigma}^{n+1} = f_\kappa^{n+1} m(\kappa) \quad \text{for } K \in \mathcal{J}
 \tag{4.15}$$

$$u_A^{n+1} = u_B^{n+1} = u_I^{n+1} = 0, \quad \text{for } \sigma = BA \in \varepsilon_{ext},
 \tag{4.16}$$

$$w_K^0 = \varphi(K), \text{ for } K \in \mathcal{J}, \quad (4.17)$$

where $f_K^{n+1} = f(K, t^{n+1})$.

5. Numerical Experiments

Let us now present some numerical results that illustrate the behavior of the proposed finite volume scheme.

The scheme (2.36)–(2.37) or (4.15)–(4.17), MPFA and the scheme in Li et al. (1980) lead to a nonsymmetric system. The scheme in Hermeline (2000) and Yuan and Sheng (2007) leads to a symmetric system. The symmetric linear systems are solved by the conjugate gradient method. The nonsymmetric linear system is solved by the biconjugate gradient stabilized algorithm (see, Saad, 1996).

Let Ω be the unit square and let $\partial\Omega_S, \partial\Omega_E, \partial\Omega_N, \partial\Omega_W$ be the boundaries of Ω . The first distorted mesh is a random mesh (e.g., Huang and Kappen, 1998). The random mesh over the physical domain $\Omega = [0, 1] \times [0, 1]$ is defined by

$$x_{ij} = \frac{i}{I} + \frac{\sigma}{I}(R_x - 0.5), \quad y_{ij} = \frac{j}{J} + \frac{\sigma}{J}(R_y - 0.5),$$

where $\sigma \in [0, 1]$ is a parameter and R_x and R_y are two normalized random variables. The second distorted mesh is a smooth mesh given by the transformation

$$x(\xi, \eta) = \xi + a_0 \sin(2\pi\xi) \sin(2\pi\eta), \quad y(\xi, \eta) = \eta + a_0 \sin(2\pi\xi) \sin(2\pi\eta).$$

Figure 6 displays a random mesh generated with $\sigma = 0.7$ and a smooth mesh generated with $a_0 = 0.1$. The scale of coarsest distorted quadrilateral mesh is 12×12 , the scale of finest distorted quadrilateral mesh is 192×192 , and the scale of finest regular grid is also 192×192 .

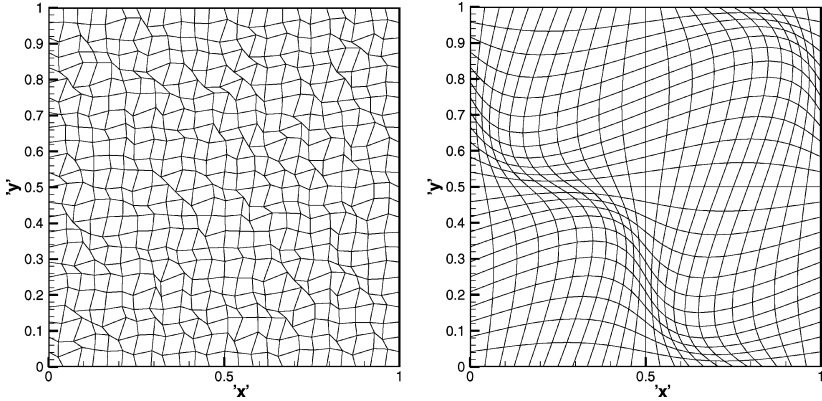


FIGURE 6 Distorted quadrilateral mesh (24×24 ; left: random mesh, right: smooth mesh).

5.1. Linear Elliptic Equation

In order to test the scheme given in Sec. 2 and compare it with the known methods, we consider following linear elliptic problem whose analytic solution is $u = 2 + \cos(\pi x) + \sin(\pi y)$:

$$\begin{aligned} -\nabla \cdot (\nabla u) &= \pi^2 (\cos(\pi x) + \sin(\pi y)) \text{ in } \Omega, \\ u &= 2 + \cos(\pi x) \text{ on } \partial\Omega_S \cup \partial\Omega_N, \\ \nabla u \cdot \nu &= 0, \text{ on } \partial\Omega_E \cup \partial\Omega_W. \end{aligned}$$

Table 1 gives the error between exact solution and computed solution on above-mentioned random meshes. From this table, we can see that our scheme is nearly second order convergence in the sense of L^∞ -norm and L^2 -norm, and is first-order convergence in the sense of H^1 -norm, which verifies the theoretical results.

Table 2 gives the error of scheme in Li et al. (1980) on random meshes. The scheme in Li et al. (1980) has only cell-center unknowns in which each cell-vertex unknown is expressed by the simple algorithmic average of neighboring cell-center unknowns. We can see clearly that this scheme fails to convergence as the number of cells is increased.

TABLE 1 Results of our scheme for the linear elliptic equation on random meshes.

$I \times J$	12×12	24×24	48×48	96×96	192×192
L^∞ -norm	1.62E-2	3.94E-3	1.11E-3	3.04E-4	8.52E-5
Rate	—	2.04	1.83	1.87	1.84
L^2 -norm	1.21E-2	3.06E-3	7.78E-4	1.97E-4	4.98E-5
Rate	—	1.98	1.97	1.98	1.99
H^1 -norm	8.31E-2	3.56E-2	1.72E-2	8.40E-3	4.13E-3
Rate	—	1.22	1.05	1.04	1.02
Time(second)	—	—	0.28	1.95	25.97

Table 3 gives the error of scheme in Hermeline (2000) on random meshes. Comparing Table 1 and 3, we can see that our scheme not only provides more accurate results than the scheme in Hermeline (2000), but it is also less expensive than it. This is because our scheme has less than half the unknowns of the scheme in Hermeline, i.e., our scheme only has the cell-center unknowns and the scheme in Hermeline has both cell-center and cell-vertex unknowns.

Table 4 gives the error of MPFA in (Aavatsmark, 2002) on random meshes. Comparing Table 1 and 4, we can see that MPFA is more accurate than our scheme in the sense of L^∞ -norm; however, our scheme is more accurate than MPFA in the sense of L^2 -norm and H^1 -norm.

In order to further compare our scheme with MPFA, we give the error of our scheme and MPFA on smooth meshes in Tables 5 and 6, respectively. We can see clearly that our scheme is more

TABLE 2 Results of the scheme in Li et al. (1980) for the linear elliptic equation on random mesh.

$I \times J$	12×12	24×24	48×48	96×96	192×192
L^∞ -norm	0.23	0.15	0.14	0.14	0.14
Rate	—	0.62	0.10	0.00	0.00
L^2 -norm	0.15	0.12	0.11	0.12	0.12
Rate	—	0.32	0.13	-0.13	0.00
H^1 -norm	0.49	0.51	0.45	0.48	0.48
Rate	—	0.06	0.18	-0.10	0.00
Time (second)	—	—	0.28	2.83	33.19

TABLE 3 Results of the scheme in Hermeline (2000) for the linear elliptic equation on random mesh.

$I \times J$	12×12	24×24	48×48	96×96	192×192
L^∞ -norm	1.67E-2	4.28E-3	1.25E-3	3.42E-4	9.31E-5
Rate	—	1.96	1.77	1.92	1.82
L^2 -norm	1.35E-2	3.42E-3	8.59E-4	2.14E-4	5.58E-5
Rate	—	1.98	1.99	2.00	1.94
H^1 -norm	1.24E-1	5.28E-2	2.51E-2	1.24E-2	6.12E-3
Rate	—	1.23	1.07	1.01	1.02
Time(second)	—	—	0.40	3.63	57.94

accurate than MPFA in the sense of L^∞ -norm and L^2 -norm. Moreover, the convergence order of our scheme in the sense of H^1 -norm is almost 1.5.

5.2. Linear Elliptic Equation with Discontinuous Coefficients

Consider the following linear elliptic problem with discontinuous coefficients

$$\begin{aligned} -\nabla \cdot (\kappa(x, y) \cdot \nabla u) &= f(x, y) \quad \text{in } \Omega, \\ u(x, y) &= 0 \quad \text{on } \partial\Omega, \end{aligned}$$

where

$$\kappa(x, y) = \begin{cases} 4, & (x, y) \in \left(0, \frac{2}{3}\right] \times (0, 1) \\ 1, & (x, y) \in \left(\frac{2}{3}, 1\right) \times (0, 1), \end{cases}$$

TABLE 4 Results of MPFA for the linear elliptic equation on random mesh.

$I \times J$	12×12	24×24	48×48	96×96	192×192
L^∞ -norm	1.49E-2	3.58E-3	1.05E-3	2.72E-4	6.99E-5
Rate	—	2.06	1.77	1.95	1.96
L^2 -norm	1.26E-2	3.09E-3	7.99E-4	1.99E-4	5.01E-5
Rate	—	2.03	1.95	2.01	1.99
H^1 -norm	8.53E-2	3.59E-2	1.76E-2	8.64E-3	4.27E-3
Rate	—	1.25	1.03	1.03	1.01
Time(second)	—	—	0.30	2.02	24.55

TABLE 5 Results of our scheme for the linear elliptic equation on smooth mesh.

$I \times J$	12×12	24×24	48×48	96×96	192×192
L^∞ -norm	1.61E-2	3.84E-3	9.38E-4	2.36E-4	5.81E-5
Rate	—	2.07	2.03	1.99	2.02
L^2 -norm	1.46E-2	3.68E-3	9.27E-4	2.32E-4	5.81E-5
Rate	—	1.99	1.99	2.00	2.00
H^1 -norm	7.11E-2	2.46E-2	8.40E-3	2.89E-3	1.01E-3
Rate	—	1.53	1.55	1.54	1.52

and

$$f(x, y) = \begin{cases} 20\pi^2 \sin \pi x \sin 2\pi y, & (x, y, t) \in (0, \frac{2}{3}] \times (0, 1) \\ 20\pi^2 \sin 4\pi x \sin 2\pi y, & (x, y, t) \in (\frac{2}{3}, 1] \times (0, 1) \end{cases}.$$

The exact solution of the problem is

$$u(x, y, t) = \begin{cases} \sin \pi x \sin 2\pi y, & (x, y, t) \in (0, \frac{2}{3}] \times (0, 1) \\ \sin 4\pi x \sin 2\pi y, & (x, y, t) \in (\frac{2}{3}, 1] \times (0, 1) \end{cases}.$$

Since κ is discontinuous at $x = 2/3$, we use the randomly distorted mesh shown in Figure 7. Hence each mesh cell is homogeneous, but material properties may vary between cells. Table 7 gives the error of our scheme on the randomly distorted meshes. From this table, one can see that our scheme has nearly second order convergence in the sense of L^∞ -norm and L^2 -norm, and has first order convergence in the sense of H^1 -norm, which verifies our theoretical results. Table 8 gives the error of scheme in Yuan

TABLE 6 Results of MPFA for the linear elliptic equation on smooth mesh.

$I \times J$	12×12	24×24	48×48	96×96	192×192
L^∞ -norm	1.86E-2	4.83E-3	1.23E-3	3.08E-4	7.70E-5
Rate	—	1.94	1.97	2.00	2.00
L^2 -norm	1.59E-2	4.06E-3	1.02E-3	2.55E-4	6.38E-5
Rate	—	1.97	1.99	2.00	2.00
H^1 -norm	7.20E-2	2.44E-2	8.34E-3	2.88E-3	1.01E-3
Rate	—	1.56	1.55	1.54	1.51

TABLE 7 Results of our scheme for the linear elliptic equation with discontinuous coefficients

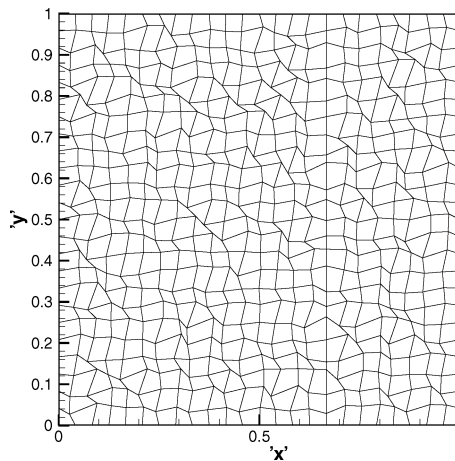
$I \times J$	12×12	24×24	48×48	96×96	192×192
L^∞ -norm	8.54E-2	2.85E-2	9.88E-3	2.80E-3	8.16E-4
Rate	—	1.58	1.53	1.82	1.78
L^2 -norm	2.81E-2	7.35E-3	1.81E-3	4.63E-4	1.17E-4
Rate	—	1.93	2.02	1.97	1.99
H^1 -norm	5.51E-1	2.20E-1	1.01E-1	5.19E-2	2.58E-2
Rate	—	1.32	1.12	0.96	1.01
Time(second)	—	—	0.30	2.32	38.68

and Sheng (2007) on the randomly distorted mesh. Comparing Table 7 and 8, we can see that our scheme is more accurate than the scheme in Yuan and Sheng.

5.3. Two Linear Parabolic Equations

At first, consider the following linear parabolic problem whose exact solution is $u = e^{-\pi^2 t} (2 + \cos(\pi x) + \sin(\pi y))$:

$$u_t - \nabla \cdot (\nabla u) = -2\pi^2 \epsilon^{-\pi^2 t} \quad \text{in } \Omega$$

**FIGURE 7** Distorted quadrilateral mesh with material discontinuities (24×24).

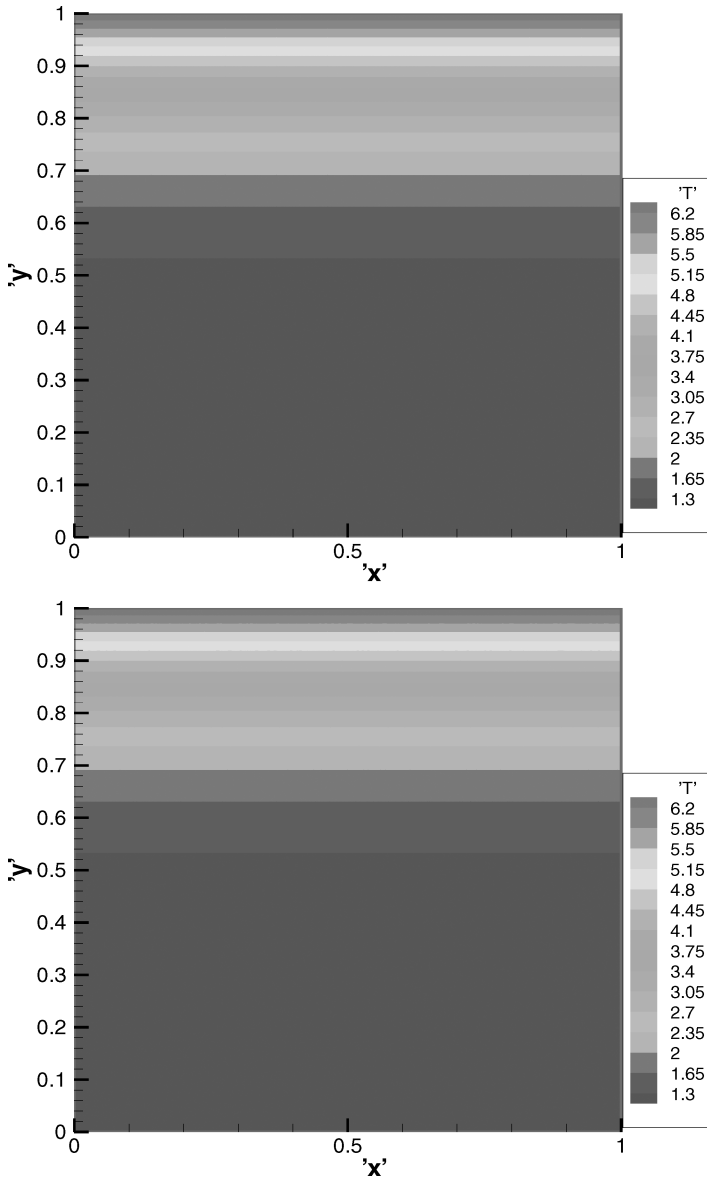


FIGURE 8 Temperature at time $t = 4 \times 10^{-2}$ (top, regular grid; bottom, distorted mesh).

TABLE 8 Results of the method in Yuan and Sheng (2007) for the linear elliptic equation with discontinuous coefficients.

$I \times J$	12×12	24×24	48×48	96×96	192×192
L^∞ -norm	1.81E-1	3.53E-2	1.12E-2	3.13E-3	8.63E-4
Rate	—	2.36	1.66	1.84	1.86
L^2 -norm	5.46E-2	1.21E-2	3.00E-3	7.43E-4	1.90E-4
Rate	—	2.17	2.01	2.01	1.97
H^1 -norm	1.24	4.20E-1	1.66E-1	7.86E-2	3.82E-2
Rate	—	1.56	1.34	1.08	1.04
Time(second)	—	—	0.32	2.48	34.00

$$u = e^{-\pi^2 t} (2 + \cos(\pi x) + \sin(\pi y)) \text{ on } \partial\Omega_S \cup \partial\Omega_N$$

$$\nabla u \cdot \nu = 0 \text{ on } \partial\Omega_E \cup \partial\Omega_W.$$

Table 9 gives the error of our scheme on random meshes. In this computation, we take $\Delta t = h_0^2$, where $h_0 = \frac{1}{J}$. From this table, we can see the similar results to stationary diffusion problem; i.e., our scheme is nearly second order convergent in the sense of L^∞ -norm and L^2 -norm, and is first order convergent in the sense of H^1 -norm. Table 10 gives the error of scheme in Hermeline (2000) on random meshes. Comparing Table 9 with 10, we can see that our scheme not only provides more accurate results than the scheme in Hermeline, but it is also less expensive than it.

Then we deal with the heat diffusion problem (see Hermeline, 2000):

$$\frac{\partial T}{\partial t} - \nabla \cdot (\kappa \nabla T) = 0 \text{ in } \Omega$$

$$T(0) = T_0 \text{ in } \Omega$$

$$\kappa \nabla T \cdot \nu + g(T - T_N) = 0 \text{ on } \partial\Omega_N$$

$$\kappa \nabla T \cdot \nu = 0 \text{ on } \partial\Omega_S \cup \partial\Omega_E \cup \partial\Omega_W.$$

TABLE 9 Results of our scheme for the linear parabolic equation on random mesh ($T = 0.1$).

$I \times J$	12×12	24×24	48×48	96×96	192×192
L^∞ -norm	5.60e-2	1.48e-2	3.68e-3	9.42e-4	2.45e-4
Rate	—	1.92	2.01	1.97	1.94
L^2 -norm	5.68E-2	1.45E-2	3.63E-3	9.08E-4	2.30E-4
Rate	—	1.97	2.00	2.00	1.98
H^1 -norm	1.12E-1	3.05E-2	9.38E-3	3.57E-3	1.60E-3
Rate	—	1.88	1.70	1.40	1.16
Time(second)	—	0.52	8.27	122.35	3801

We choose $\kappa = 1$, $g = 1$, $T_N = 30$, $T_0 = 1$, and $\Delta t = 5 \times 10^4$, and use the finest regular mesh and the finest random mesh mentioned above. Figure 8 displays the temperature at time $t = 4 \times 10^{-2}$. One can see that the contour on random mesh accords with the contour on regular mesh.

5.4. Nonlinear Parabolic Equations

Consider the following nonlinear radiation diffusion problem:

$$\begin{aligned} \frac{1}{C} \frac{\partial T}{\partial t} - \nabla \cdot (\lambda \nabla T^4) &= 0 \quad \text{in } \Omega \\ T(0) &= T_0 \quad \text{in } \Omega \\ \lambda \nabla T^4 \cdot \nu + T^4 - T_N^4 &= 0 \quad \text{on } \partial\Omega_N \\ \lambda \nabla T \cdot \nu &= 0 \quad \text{on } \partial\Omega_S \cup \partial\Omega_E \cup \partial\Omega_W, \end{aligned}$$

TABLE 10 Results of the scheme in Hermeline (2000) for the linear parabolic equation on random mesh ($T = 0.1$).

$I \times J$	12×12	24×24	48×48	96×96	192×192
L^∞ -norm	5.67E-2	1.49E-2	3.74E-3	9.54E-4	2.44E-4
Rate	—	1.93	1.99	1.97	1.97
L^2 -norm	6.58E-2	1.68E-2	4.21E-3	1.05E-3	2.66E-4
Rate	—	1.97	2.00	2.00	1.98
H^1 -norm	2.31E-1	6.17E-2	2.45E-2	1.23E-2	6.10E-3
Rate	—	1.90	1.33	0.99	1.01
Time(second)	—	0.78	12.47	178.07	5092

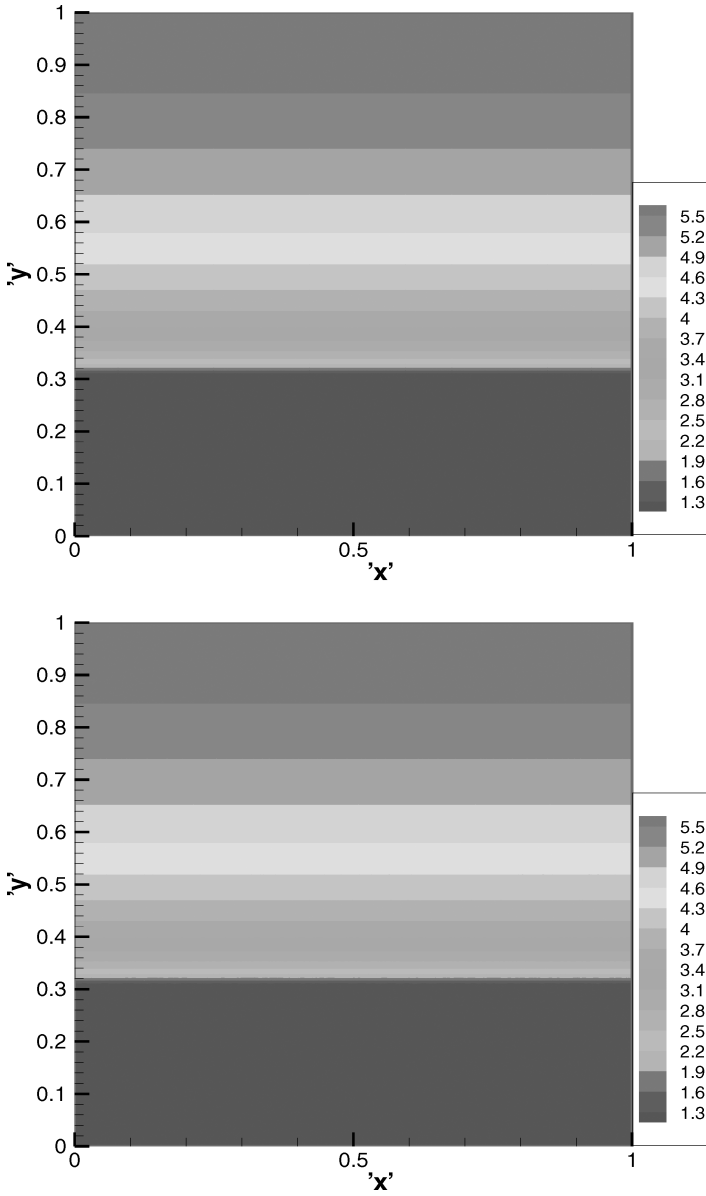


FIGURE 9 Temperature T/T_r at time $t = 5 \times 10^{-4} \lambda_r/c$ (top, regular mesh; bottom, distorted mesh).

where

$$\lambda = 1.6 \times 10^{34} \frac{1}{n^2} T^{7/2}.$$

Let $u = T^4 / T_r^4$ and $\kappa(u) = u^{7/8}$. The radiation diffusion problem above becomes (see Hermeline, 2000)

$$\begin{aligned} \frac{\partial u}{\partial t} - \nabla \cdot (\kappa(u) \nabla u) &= 0 & \text{in } \Omega \\ u(0) &= u_0 & \text{in } \Omega \\ \kappa(u) \nabla u \cdot \nu + u - u_N &= 0 & \text{on } \partial\Omega_N \\ \kappa(u) \nabla u \cdot \nu &= 0 & \text{on } \partial\Omega_S \cup \partial\Omega_E \cup \partial\Omega_W. \end{aligned}$$

We choose $u_N = 8.1 \times 10^5$, $u_0 = 1$ (hence $T_N = 30T_r$, $T_0 = T_r$), $\Delta t = 5 \times 10^{-6} t_r$, and use the finest regular mesh and the finest random mesh mentioned above. Figure 9 displays the temperature at time $t = 5 \times 10^{-4} t_r$. One can also see that the contour on random mesh accord with the contour on regular mesh.

6. Conclusion

We present a kind of new expression of cell-vertex unknowns in the nine-point scheme for discretizing diffusion operators on distorted quadrilateral meshes. Although the scheme is designed only on quadrilateral meshes, it is straightforward to extend the method to arbitrary polygon meshes. The resulting algorithm has only cell-center unknowns, and cell-vertex unknowns are eliminated by expressing them as linear combination of neighboring cell-center unknowns through the following process. Firstly we construct a special control-volume for each cell-vertex, and then device a finite volume scheme in this control-volume to obtain the linear relation between cell-vertex unknowns and cell-center unknowns. Hence cell-vertex unknowns are eliminated by expressing them as the linear weighted combination of cell-center unknowns and the discrete values of the source term. Moreover, this scheme has a local stencil, and it reduces to the standard five-point

scheme when the mesh lines are orthogonal. The arbitrary distorted meshes can be used without the numerical results being altered remarkably. Our scheme is compared with some exiting cell-centered diffusion schemes by using numerical experiments, and is shown to be nearly second order convergent in L^2 and L^∞ norms, and first order convergent in H^1 norm.

References

- Aavatsmark I. (2002). An introduction to multipoint flux approximations for quadrilateral grids. *Comput. Geosci.* 6: 404–432.
- Aavatsmark I., Eigestad G.T. (2006). Numerical convergence of the MPFA O-method and U-method for general quadrilateral grids. *Int. J. Numer. Meth. Fluids* 51: 939–961.
- Aavatsmark I., Barkve T., Bøe Ø., Mannseth T. (1998). Discretization on unstructured grids for inhomogeneous, anisotropic media. Part I: Derivation of the methods. *SIAM J. Sci. Comput* 19: 1700–1716.
- Aavatsmark I., Barkve T., Bøe Ø., Mannseth T. (1998). Discretization on unstructured grids for in-homogeneous, anisotropic media. Part II: Discussion and numerical results. *SIAM J. Sci. Comput* 19: 1717–1736.
- Breil J., Maire P.-H. (2007). A cell-centered diffusion scheme on two-dimensional unstructured meshes. *J. Comput. Phys.* 224: 785–823.
- Li D., Shui H., Tang M. (1980). On the finite difference scheme of two-dimensional parabolic equation in a non-rectangular mesh. *J. Num. Method & Comp. Appl.* 4: 217–224.
- Hermeline F. (2000). A finite volume method for the approximation of diffusion operators on distorted meshes. *J. Comput. Phys.* 160:481–499.
- Huang W., Kappen A. M. (1998). A study of cell-center finite volume methods for diffusion equations, Mathematics Research Report, 98–10-01, University of Kansas, Lawrence KS66045.
- Wu J., Fu S., Shen L. (2003). A difference scheme with high resolution for the numerical solution of nonlinear diffusion equation. *J. Num. Method & Comp. Appl.* 24: 116–128.
- Kershaw D. S. (1981). Differencing of the diffusion equation in Lagrangian hydrodynamic codes. *J. Comput. Phys.* 39:375–395.
- Klausena R. A., Russell T. F. (2004). Relationships among some locally conservative discretization methods which handle discontinuous coefficients. *Comput. Geosci.* 8: 341–377.
- Lipnikov K., Shashkov M., Svyatskiy D. (2006). The mimetic finite difference discretization of diffusion problem on unstructured polyhedral meshes, *J. Comput. Phys.* 211:473–491.
- Morel J. E., Dendy J. E., Hall M. L., White S. W. (1992). A cell centered Lagrangian-mesh diffusion differencing scheme. *J. Comput. Phys.* 103:286–299.

- Morel J. E., Roberts R. M., Shashkov M. J. (1998). A local support-operators diffusion discretization scheme for quadrilateral r - z meshes. *J. Comput. Phys.* 144: 17–51.
- Saad Y. (1996). Iterative method for sparse linear systems. PWS publishing, New York.
- Shashkov M., Steinberg S. (1995). Support-operator finite-difference algorithms for general elliptic problems. *J. Comput. Phys.* 118: 131.
- Shashkov M. (1996). Conservative finite-difference methods on general grids, CRC Press, Boca Raton, FL.
- Sheng Z., Yuan G. (2008). A Nine Point Scheme for the Approximation of Diffusion Operators on Distorted Quadrilateral Meshes. *SIAM J. Sci. Comput.* 30: 1341–1361.
- Yuan G., Sheng Z. (2007). Analysis of accuracy of a finite volume scheme for diffusion equations on distorted meshes. *J. Comput. Phys.* 224:1170–1189.